

Stable-isotope tracing of vadose-zone water transport in *Achnatherum splendens* grassland of the Qinghai Lake Basin, NE Qinghai–Tibet Plateau, China

Bao-Fu Jiang^a, Bu-li Cui^{a,b,c,*}, Ying Wang^a, Ya-Xuan Wang^a, Dong-sheng Li^a, Long-sheng Wang^a, Xiao-Yan Li^b

^a School of Resources and Environmental Engineering, Ludong University, Yantai 264025, China

^b School of Natural Resources, Faculty of Geographical Science, Beijing Normal University, Beijing 100875, China

^c State Key Laboratory of Loess and Quaternary Geology, Institute of Earth Environment, Chinese Academy of Sciences, Xi'an 710061, China

ARTICLE INFO

Keywords:

Vadose zone
Water transport
Stable-isotope tracing
Achnatherum splendens grassland
Qinghai Lake Basin

ABSTRACT

The vadose zone serves as a connection and transformation link between the atmosphere, plants, soil, surface water and groundwater. It is considered to be an important component of the geosphere and has sensitive interactions with the hydrosphere, biosphere, and atmosphere, which greatly impacts the environment and human health. This study was conducted in the *Achnatherum splendens* grassland of the Qinghai Lake Basin, NE Qinghai–Tibet Plateau, China, and can provide references and guidance for research on the mechanisms governing the circulation and evolution of vadose-zone water in cold arid regions. Precipitation, dustfall, and vadose zone samples were collected to investigate transport in the vadose zone water using stable isotopes of hydrogen ($\delta^2\text{H}$) and oxygen ($\delta^{18}\text{O}$) as well as chloride as environmental tracers. The results showed that precipitation was the main source of chloride in the research area, accounting for 86.5% of total chloride deposition. The soil water in the vadose zone was mainly recharged by local precipitation. Strong evaporation occurred before the precipitation infiltrated and recharged soil water. The soil water, chloride content, and isotope values in the soil profile varied across different depths. The annual potential recharge from precipitation to the vadose zone soil water was 9.20 mm/yr, accounting for 2.17% of the local precipitation. The actual recharge from precipitation to groundwater was 26.29 mm/yr, accounting for 6.19% of the local precipitation. The infiltration recharge from preferential and piston flow accounted for 66.40% and 33.60% of the total infiltration recharge to groundwater, respectively, indicating that preferential flow was the main source of groundwater recharge in the studied grassland. The results of this study were compared with those of other relevant studies. The recharge mechanisms of the vadose zone soil water and groundwater varied between different regions and were controlled mainly by the spatiotemporal distribution of precipitation, topographic characteristics, and soil structure. These findings provide a reference and guidance for research on the circulation and evolution of vadose-zone water in the Qinghai Lake Basin and Qinghai–Tibet Plateau.

1. Introduction

The vadose zone is a connection and transformation link between the atmosphere, plants, soil, surface water, and groundwater that serves as a carrier for the transport and reaction of various chemical substances (Herczeg and Leaney, 2011; Gao et al., 2014; Huang et al., 2016). This zone is considered to be an important component of the geosphere and has sensitive interactions with the hydrosphere, biosphere, and

atmosphere. Thus the vadose zone significantly influences the environment and human health (Ma et al., 2004; Scanlon et al., 2010; Liu et al., 2012). Soil water in the vadose zone plays an intermediate role in the infiltration and transformation of precipitation into groundwater (Scanlon et al., 2006; Tan et al., 2016). The vadose zone is a direct water source for plant roots (Favreau et al., 2009; Reck et al., 2018). It is an essential component in the formation, transformation, and consumption of water resources, and its dynamics directly affect various hydrological

* Corresponding author at: School of Resources and Environmental Engineering, Ludong University, No. 186 Hongqizhong Street, Yantai, Shandong 264025, China.

E-mail address: cuibuli@163.com (B.-l. Cui).

processes, such as flood processes, soil erosion, solute transport, land-air interactions, groundwater recharge and discharge, and landform and soil formation processes (Goldin, 2016; Bashir and Chevez, 2018; Li et al., 2018; Reck et al., 2018).

Therefore, the formation, influencing factors, and transport patterns of vadose-zone water are of great research interest and relevance to various disciplines, such as hydrology, soil science, and ecology (Baran et al., 2007; Herczeg and Leaney, 2011; Gleeson et al., 2016; Bashir and Chevez, 2018; Li et al., 2018; Reck et al., 2018). Research on the spatiotemporal dynamics and transport patterns of vadose-zone water is of theoretical and practical significance for the rational exploitation of water resources, maintenance of water-soil balance, prevention of land desertification and vegetation degradation, and maintenance of ecological health (Bashir and Chevez, 2018; Zhu et al., 2019). Such research can reveal the formation, recharge, and evolution mechanism of groundwater to ensure a balance between groundwater exploitation and recharge and to achieve optimal allocation of groundwater resources (Gleeson et al., 2016; Huang et al., 2016).

Long-term and continuous observations are required to reveal the transport pattern of vadose-zone water, and related research has primarily been conducted in arid or temperate climate zones (Ma et al., 2004; Lin et al., 2013; Huang et al., 2016). Few experiments have been conducted in cold arid regions with harsh field conditions. Accordingly, this gap in knowledge on the transport pattern of vadose-zone soil water in cold arid regions must be addressed by research on hydrological cycles (e.g., mutual transformation between surface, soil, and groundwater) and ecohydrological processes (Li et al., 2018).

The Qinghai Lake Basin is located in the alpine and semi-arid region of the northeastern Qinghai-Tibet Plateau, China, and occupies an area of 29,661 km². The basin contains China's largest inland saltwater lake, Qinghai Lake (with a water area of 4264 km²). Qinghai Lake is not only an important water body for ecological security in the northeastern Qinghai-Tibet Plateau but also a national nature reserve with internationally important wetlands (Tang et al., 1992). Furthermore, the Qinghai Lake Basin is a key area for socioeconomic development, such as ecotourism and grassland husbandry in Qinghai Province. However, water resources in the basin have been declining because of climate change and human activity, which have resulted in various environmental problems, such as grassland degradation, wetland reduction, and decreased biodiversity, which have raised international concern (Li et al., 2007; Xin, 2008).

Grassland (vegetation) degradation, wetland reduction, and desertification in the Qinghai Lake Basin are closely related to changes in the soil water content (vadose-zone water) and groundwater levels (Zhang et al., 2006; Xin, 2008; Zhao et al., 2013). Therefore, research on the transport pattern and recharge cycle of vadose-zone water is necessary to understand ecological degradation in the basin and the interaction between the vadose zone and groundwater. Such research can further reveal the groundwater recharge and circulation pattern in the Qinghai Lake Basin, which has practical significance for predicting and regulating water resources in the basin and protecting the environment and human health.

The widespread application of isotopic analysis in hydrology has provided an effective means for the identification of water transport processes in the vadose zone (Clark and Fritz, 1997; Edmunds and Tyler, 2002; Scanlon et al., 2007; Herczeg and Leaney, 2011; Liu et al., 2012; Huang et al., 2016). Isotopes in water bodies participate in the entire water circulation process, serving as natural tracers for identifying the water sources and hydrological transformation processes. These isotopes are thus referred to as the "fingerprint" or "DNA" of water (Clark and Fritz, 1997; Kendall and McDonnell, 1998; Gu et al., 2011). The combination of isotopes and hydrochemical methods can reveal the formation and evolution mechanisms of various water bodies (Xu et al., 2006; Baran et al., 2007; Hou et al., 2008; Wang et al., 2009; Adomako et al., 2010; Liu et al., 2012; Huang et al., 2016). Therefore, groundwater research has increasingly focused on the transport of vadose-zone water

by jointly using isotope and traditional hydrogeological methods (Gibson et al., 2005; IAEA, 2013; Ye and Chang, 2019).

This study selected the *Achnatherum splendens* grassland in the Qinghai Lake Basin as the research area to sample and monitor precipitation, dustfall, and vadose-zone water. We employed stable-isotope tracer technology and numerical simulations to investigate the transport of vadose zone water in the grassland. The objectives of the study were to (1) determine the temporal characteristics of precipitation isotope values and atmospheric chloride deposition in the Qinghai Lake Basin, (2) reveal the redistribution and transport mechanism of precipitation during infiltration through the vadose zone, and (3) estimate the quantity and time required for vertical recharge from precipitation to vadose-zone soils and groundwater. The results not only provide basic data for quantitative research on water circulation processes and transformation in the Qinghai Lake Basin but also provide references and guidance for research on the mechanisms governing the circulation and evolution of vadose-zone water in cold arid regions.

2. Study area

The Qinghai Lake Basin (36°15'–38°20' N, 97°50'–101°20' E) is located on the northeastern Qinghai-Tibet Plateau (Fig. 1). It lies at the intersection between the East Asian monsoon region, the northwest arid region, and the high cold region of the Qinghai-Tibet Plateau, with a semi-arid temperate continental climate (Cui and Li, 2015). The annual mean temperature in the basin is 0.39 °C, and the temperature decreases from the southeast to the northwest. The annual mean precipitation is approximately 375 mm, with large seasonal variations. Dry and cold northwesterly air flow prevails in winter with little precipitation. In summer, the basin receives warm and humid southwesterly air flow from the western Pacific Ocean, and the precipitation during this season accounts for approximately 70% of the annual precipitation. The basin experiences a high evaporation rate in normal years, with an annual mean evaporation of 1500 mm (Li et al., 2007; Cui and Li, 2016).

The *A. splendens* grassland is distributed throughout the Qinghai Lake Basin and accounts for approximately one-third of the area around Qinghai Lake. The research area was located at the Qinghai Sanjiaocheng Sheep Breeding Farm on the northern side of Qinghai Lake (Fig. 1), where *A. splendens* is the predominant vegetation. Other vegetation includes *Convolvulus ammannii*, *Artemisia sieversiana*, *Astragalus* sp., *Stipa krylovii*, *Stipa breviflora*, *Allium tanguticum*, *Dracocephalum heterophyllum*, and *Pedicularis* sp. (Zhou et al., 2003). The soils in the research area are dominated by chestnut soil, which is characterized by high dryness and sandiness. Soil salt accumulation is present in some areas (Wu et al., 2015). The average soil bulk density is 1.21 g/cm³, the field soil water-holding capacity is 30.5%, and the maximum frozen soil depth is 2.90 m. Soils at different depths have nearly the same particle composition: approximately 10% clay, 50% silt, and 40% sand (Chen et al., 2008). The depth of the groundwater table is 4–5 m.

3. Data and methods

3.1. Sample collection and testing

From July 2018 to June 2019, a precipitation sampling device was deployed at the Meteorological Bureau of Gangcha County (Fig. 1), where a total of 136 precipitation samples—104 rain, 8 snow, and 24 sleet—were collected. A dustfall sampling device was deployed in the *A. splendens* grassland of the Qinghai Lake Basin and sampling was performed once a month, when a total of 12 dustfall samples were collected.

Soil profile samples of the vadose zone were collected from representative sites in the *A. splendens* grassland. The soil profile consisted of humus (0–5 cm), leaching (5–80 cm), illuvial (80–100 cm), and parent material (100–400 cm) horizons (Fig. 2). Vadose-zone soil samples were collected on a quarterly basis at profile depths of 0–400 cm (Fig. 2)

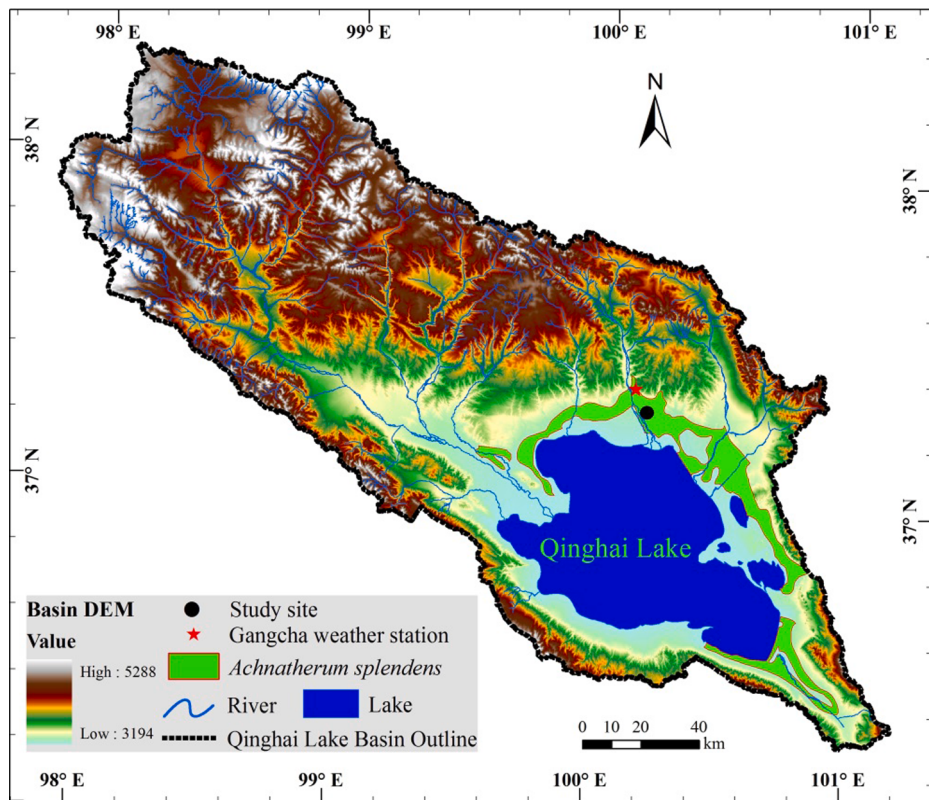


Fig. 1. Location of the Qinghai Lake Basin in China and sampling sites.

divided into 14 layers: 0–10 cm (S1), 10–20 cm (S2), 20–30 cm (S3), 30–40 cm (S4), 40–60 cm (S5), 60–80 cm (S6), 80–100 cm (S7), 100–140 cm (S8), 140–180 cm (S9), 180–220 cm (S10), 220–260 cm (S11), 260–300 cm (S12), 300–350 cm (S13), and 350–400 cm (S14). The sample collection dates were July 20, 2018 (summer), November 27, 2018 (autumn), February 26, 2019 (winter), and May 28, 2019 (spring). Groundwater samples were collected near the soil profile. Soil bulk density, particle size, and water content were measured at the field observation station of Beijing Normal University in the basin. Hydrogen and oxygen stable isotope values ($\delta^{2}\text{H}$ and $\delta^{18}\text{O}$, respectively) of precipitation, soil water, and groundwater were measured using a Los Gatos Research liquid water isotope analyzer (IWA-45-EP). The measurement accuracy of $\delta^{2}\text{H}$ and $\delta^{18}\text{O}$ values was $\pm 0.5\%$ and $\pm 0.1\%$, respectively. The chloride content of precipitation, soil water, and groundwater was measured at Ludong University using ion chromatography (Dionex 600) and the repeated sampling error was 0.5–1% (2σ).

3.2. Research methods

In this study, the chloride mass balance (CMB) method was adopted to estimate the recharge of precipitation to vadose-zone water. The CMB method is based on the inertness of chloride. The high solubility of chloride means that it is not readily involved in geochemical interactions, even at high concentrations, when it can still be co-transported with water molecules through the vadose zone. Moreover, chloride is not volatile and is thus retained in the vadose zone despite evapotranspiration. Its concentration is directly proportional to the amount of water removed by evapotranspiration, making it the most stable tracer for vadose-zone water (Allison and Hughes, 1983). The differences between the chloride concentration of soil water and precipitation water can reflect the amount of effective precipitation infiltration and historical dynamics of precipitation infiltration (Scanlon et al., 2006; Huang et al., 2016).

3.2.1. Potential recharge of precipitation into the vadose-zone

According to the law of conservation of mass, the amount of precipitation and concentration of chloride therein have the following relationship with the amount of infiltration and chloride concentration of soil water:

$$P^*Cl_p = R^*Cl_{sw} \quad (1)$$

$$R_s = P^*Cl_p / Cl_{sw} \quad (2)$$

where P is the annual precipitation (mm/yr); Cl_p is the mass concentration of chloride in precipitation (mg/L); R_s is the potential amount of precipitation infiltration (mm/yr); and Cl_{sw} is the mass concentration of chloride in the vadose-zone soil water (mg/L). The latter is usually measured using the soil water beneath plant root zones considering that solutes in the surface and root-zone soil water are enriched because of evaporation and plant absorption, whereas enrichment usually does not take place beneath plant root zones. Given that the root zone depth of *A. splendens* and other plants in the research area was approximately 100 cm, the chloride content of soil water at depths of 100–260 cm was measured to calculate the amount of recharge from precipitation (Edmunds and Tyler, 2002; Huang et al., 2016).

3.2.2. Actual recharge of precipitation to groundwater

The chloride mass balance method was employed to calculate the actual recharge (Gleeson et al., 2016). The equation is similar to Eq. (2) except for the substitution of Cl_{sw} with the mean chloride concentration in groundwater Cl_{gw} .

$$R_g = P^*Cl_p / Cl_{gw} \quad (3)$$

where P is the annual precipitation (mm/yr); Cl_p is the mass concentration of chloride in precipitation (mg/L); R_g is the recharge amount of precipitation to groundwater (mm/yr); and Cl_{gw} is the mass concentration of chloride in the groundwater (mg/L).

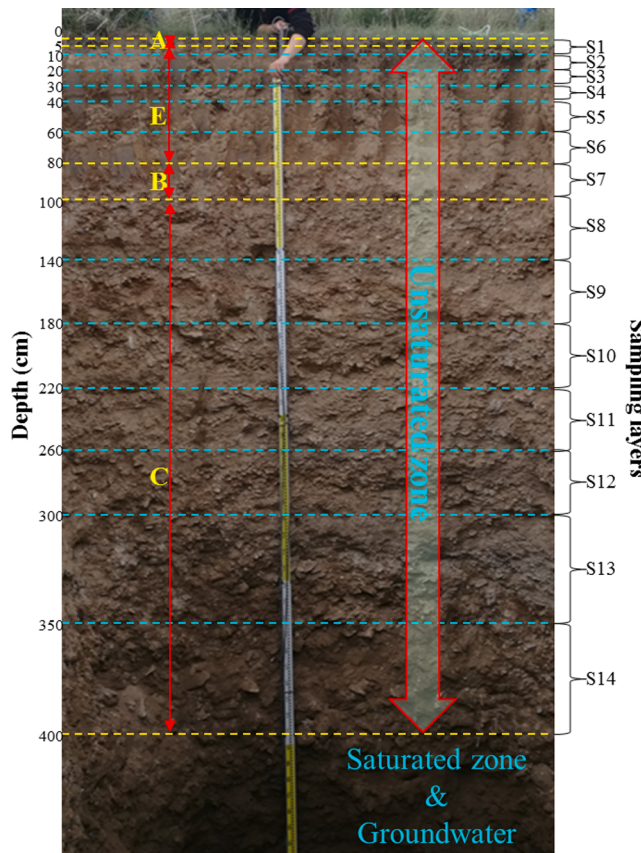


Fig. 2. Soil characteristics and sampling depth of soil profile. Soil characteristics: Humus layer (0–5 cm), eluvial layer (5–80 cm), illuvial layer (80–100 cm), parent material layer (100–400 cm); Sampling layers: 0–10 cm (S1), 10–20 cm (S2), 20–30 cm (S3), 30–40 cm (S4), 40–60 cm (S5), 60–80 cm (S6), 80–100 cm (S7), 100–140 cm (S8), 140–180 cm (S9), 180–220 cm (S10), 220–260 cm (S11), 260–300 cm (S12), 300–350 cm (S13), and 350–400 cm (S14).

Groundwater originates from multiple components, including the piston and preferential flows. To calculate the contribution of the piston and preferential flows to groundwater, according to the mass conservation law, the total recharge amount R_g can be expressed as follows:

$$R_g = R_{pr} + R_{sw} \quad (4)$$

$$R_g * Cl_{gw} = R_{pr} * Cl_{pr} + R_{sw} * Cl_{sw} \quad (5)$$

where R_{pr} is the recharge amount contributed by preferential flow (mm/yr); R_{sw} is the recharge amount contributed by piston flow (mm/yr); Cl_{gw} is the chloride concentration of groundwater (mg/L); Cl_{pr} is the chloride concentration of preferential flow (mg/L); and Cl_{sw} is the chloride concentration of the piston flow (mg/L). If Cl_{sw} is similar to Cl_{gw} , the piston flow can be considered to be the only contributor to recharge. If Cl_{sw} is much higher than Cl_{gw} , there may be a preferential flow component, and a dual recharge process is possible (Sharma and Hughes, 1985). In this study, Cl_{pr} was assumed to be equal to the chloride content of precipitation (mg/L), and Cl_{sw} was measured as the chloride content of soil water at profile depths of 100–260 cm (depths at which chloride content increases significantly and the diluting effect of precipitation is negligible; mg/L).

$$f(R_{pr}) = (Cl_{sw} - Cl_{gw}) / (Cl_{sw} - Cl_{pr}) \quad (6)$$

$$f(R_{sw}) = 1 - f(R_{pr}) \quad (7)$$

4. Results and discussion

4.1. Isotope characteristics of precipitation

The $\delta^2\text{H}$ values of precipitation in the Qinghai Lake Basin were between $-183.51\text{\textperthousand}$ and $17.75\text{\textperthousand}$ (with an average of $-70.27\text{\textperthousand}$), whereas the range and average of $\delta^{18}\text{O}$ values were $-25.18\text{--}0.48\text{\textperthousand}$ and $-10.59\text{\textperthousand}$, respectively. Both $\delta^2\text{H}$ and $\delta^{18}\text{O}$ values were within the reported ranges for precipitation across China ($\delta^2\text{H}$: $-28\text{--}24\text{\textperthousand}$; $\delta^{18}\text{O}$: $-35.5\text{--}2.5\text{\textperthousand}$) (Tian et al., 2001). To define a local water line, more than 1 year of data is required. The plot of $\delta^2\text{H}$ versus $\delta^{18}\text{O}$ for precipitation constituted the local meteoric water line (LMWL) of the Qinghai Lake Basin, namely $\delta^2\text{H} = 7.95\delta^{18}\text{O} + 11.98$ (Fig. 3). The LMWL deviated slightly from the global meteoric water line (GMWL), which was attributed to the unique local circulation system of the Qinghai Lake Basin with multiple water vapor sources and different evaporation patterns at different spatiotemporal scales. The slope of the LMWL was lower than that of the GMWL. This indicates that the precipitation processes in the basin were affected by below-cloud secondary evaporation (Liu et al., 2008; Gui et al., 2019).

Hydrogen and oxygen stable isotopes of precipitation were relatively enriched in summer and depleted in winter (Fig. 3). These patterns are consistent with those of local temperatures, indicating that the $\delta^2\text{H}$ and $\delta^{18}\text{O}$ values of precipitation in the Qinghai Lake Basin were affected by temperature. Similar effects have been observed in Delhi (India), Urumqi, Zhangye (western China), and other arid regions of central Asia (Tian et al., 2001; Yu et al., 2008; Liu et al., 2008).

4.2. Deposition characteristics of atmospheric chloride

Twelve atmospheric deposition samples were collected from July 2018 to June 2019 with a total mass of 279.35 g/m^2 for the whole year, which was similar to that of dustfall collected around Qinghai Lake ($265.7 \pm 55.0\text{ g/m}^2$) by Wan et al. (2012) and those collected in nearby areas by Gao et al. (2013). The monthly mass of dustfall samples varied from 2.71 to 64.16 g/m^2 and tended to increase gradually from January to August and decrease gradually from August to December. The highest deposition occurred in summer, the second highest in early autumn, and the lowest in winter (Fig. 4). Dissolution testing revealed that the yearly and monthly total deposition mass of chloride were 1321.13 mg/m^2 and $14.56\text{--}317.97\text{ mg/m}^2$, respectively (Fig. 5). Chloride showed a similar monthly trend in deposition mass as that of the dustfall samples throughout the year, that is, the deposition gradually increased from January to August and gradually decreased from August to December.

The total chloride deposited throughout the year included that deposited by precipitation (1149.70 mg/m^2) and dustfall (179.94 mg/m^2). Precipitation chloride accounted for 86.5% of the total chloride deposition (Fig. 6), indicating that precipitation was the main source of chloride in the area. The monthly deposition of precipitation chloride ranged from 0.44 to 304.96 mg/m^2 and exhibited seasonal variations, gradually increasing from January to August then gradually decreasing from August to December. This was consistent with the trend in monthly precipitation, indicating that the amount of deposited precipitation chloride was mainly determined by the amount of precipitation (Fig. 6). The monthly deposition of dustfall chloride was $13.00\text{--}17.79\text{ mg/m}^2$, and it showed little variation, being lower in summer and higher in other seasons (Fig. 6).

The area surrounding the Qinghai Lake Basin in the northeastern Qinghai-Tibet Plateau is sparsely populated, with few mineral exploitation activities and factories. Therefore, the dustfall and deposited chloride in the basin originated mainly from dust carried by airflow, chloride carried by water vapor masses, and locally generated dust (Wan et al., 2012). Moreover, the Qinghai Lake Basin is located in the hinterland of the Eurasian continent, at the intersection of the East Asian monsoon region, northwestern arid region, and high cold region of the Qinghai-Tibet Plateau, with southeasterly monsoons from June to

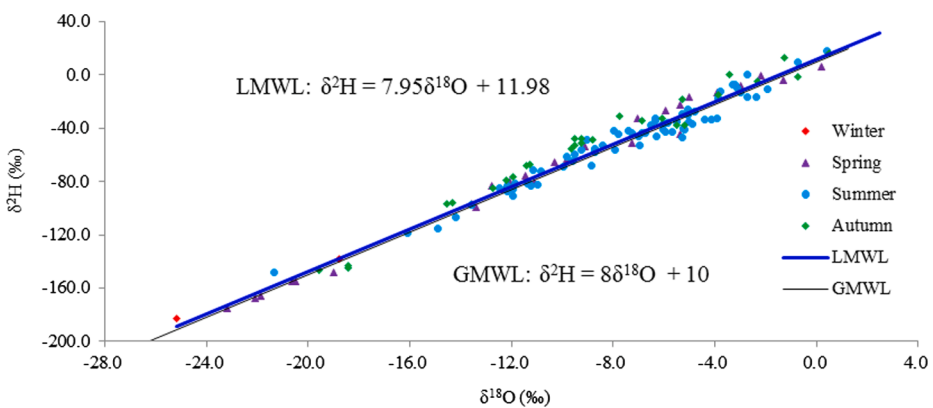


Fig. 3. Relationship between $\delta^2\text{H}$ and $\delta^{18}\text{O}$ of precipitation. LMWL, Local meteoric water line; GMWL, Global meteoric water line.

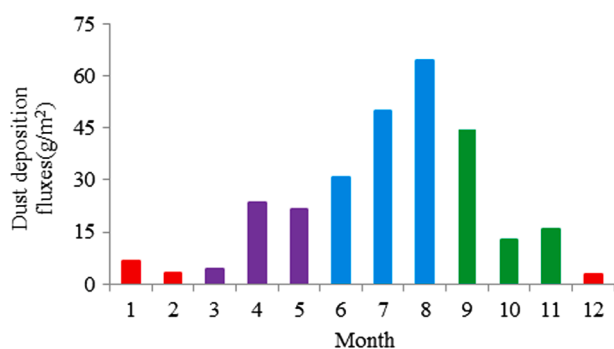


Fig. 4. Monthly dust deposition fluxes. winter: red; spring: purple; summer: blue; autumn: green. (For interpretation of the references to colour in this figure legend, the reader is referred to the web version of this article.)

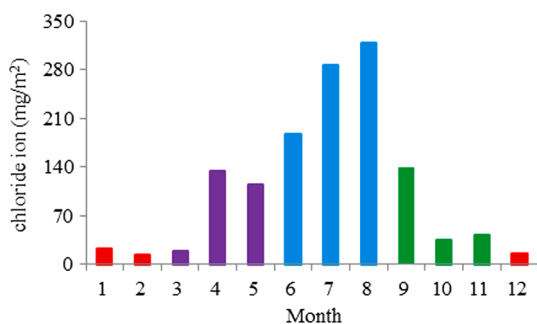


Fig. 5. Monthly chloride content in dust deposition fluxes. winter: red; spring: purple; summer: blue; autumn: green. (For interpretation of the references to colour in this figure legend, the reader is referred to the web version of this article.)

August and westerly winds from September to May (Cui and Li, 2015). Precipitation in the Qinghai Lake Basin is concentrated mainly in summer (62.17%), when the diluting effect of precipitation leads to relatively low dustfall chloride.

4.3. Changes of chloride and stable isotopes in vadose-zone soil water

As shown in Fig. 7, the content of vadose-zone soil water exhibited three distinctive trends over three profile depth ranges: (1) 0–100 cm, where the water content decreased with increasing depth, from 20.42% in the surface layer to 6.60% in the bottom layer; (2) 100–300 cm, where the water content fluctuated with increasing depth (average of 3.32%); and (3) 300–400 cm, where the water content increased from 3.57% to 5.55% with increasing depth. These indicate that surface soil water

content was greatly affected by plant roots and precipitation, and it gradually decreased with increasing depth (Zhou et al., 2003). Soil water content at deeper depths (about 400 cm) was greatly affected by capillary forces and groundwater (groundwater table depth varied between 406 and 500 cm), and it gradually increased with increasing soil profile depth. The vadose zone soil water content varied seasonally, being highest in summer, followed by that in autumn and spring, and was the lowest in winter, especially at profile depths of 0–100 cm. This was mainly because local precipitation was concentrated in summer and autumn (Fig. 6), which greatly affected the surface soil water (Cui and Li, 2015). Soil water content at depths greater than 350 cm in different seasons decreased in the following order: spring > winter > autumn > summer; the groundwater table depths were 406, 437, 465, and 500 cm, respectively, which indicated that the deep soil water content was mainly affected by fluctuations in the depth of the groundwater table.

The chloride content of soil water at different soil profile depths ranged from 48.12 to 544.28 mg/L, characterized by three distinctive trends over three profile depth ranges (Fig. 8). That is, the chloride content gradually increased with increasing depth at 0–40 cm, from 48.12 mg/L to 255.31 mg/L. The chloride content was the highest at 40–100 cm, averaging 490.48 mg/L, and was relatively stable; it tended to decrease from 146.15 to 51.68 mg/L at 100–400 cm, approaching the chloride content of groundwater (50.25 mg/L). The depth distribution and trends of the chloride content of soil water in this study were typical of arid and semi-arid regions (Allison and Hughes, 1983; Huang et al., 2016; Lu et al., 2020). The gradual increase in the chloride content of soil water with increasing soil profile depth (0–40 cm) was mainly attributed to the fact that precipitation leached the surface soil, resulting in a lower chloride content in the upper layers (Huang et al., 2016). The chloride content was high at depths of 40–100 cm and reached a maximum at 80 cm, mainly because water absorption by plant roots caused chloride accumulation at this depth (Li et al., 2017). The chloride content at depths greater than 100 cm was diluted and tended to stabilize (Fig. 8). The decreasing degree of enrichment in the soil profile could be attributed to two factors: (1) the evaporation intensity of soil water gradually decreased with increasing soil depth in the vadose zone, and (2) plant absorption gradually decreased with increasing soil depth in the vadose zone. Deep soil water (approximately 400 cm) was greatly affected by the groundwater, and there was a hydraulic connection between deep soil water and groundwater. Therefore, the chloride content of deep soil water approached that of groundwater. The chloride content of soil water at soil depths of 0–100 cm showed seasonal variation, decreasing in the following order: summer > autumn > winter > spring. This was mainly attributed to vigorous plant growth in summer and autumn (Li et al., 2017), when plant roots absorbed a large amount of soil water, which concentrated chloride to a greater extent than during winter and spring. At soil profile depths of more than 100 cm, the chloride content of soil water was lower in summer than in spring and

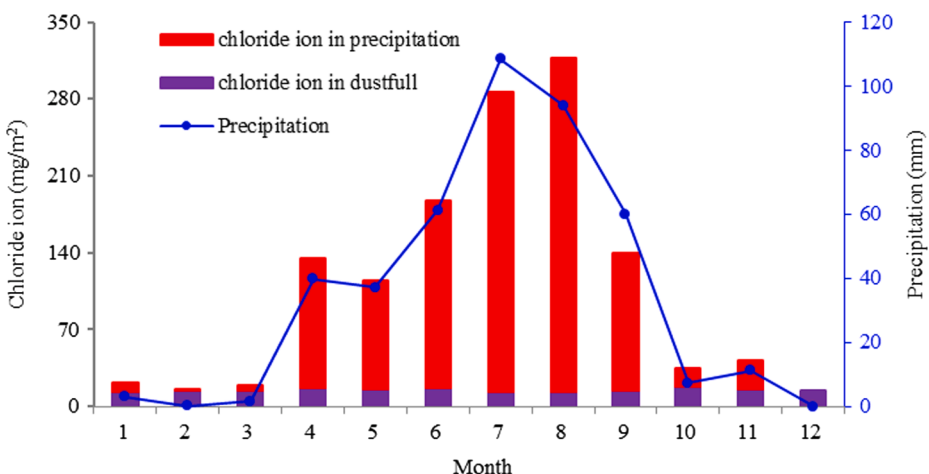


Fig. 6. Monthly chlorine ion levels in observed dustfall and precipitation.

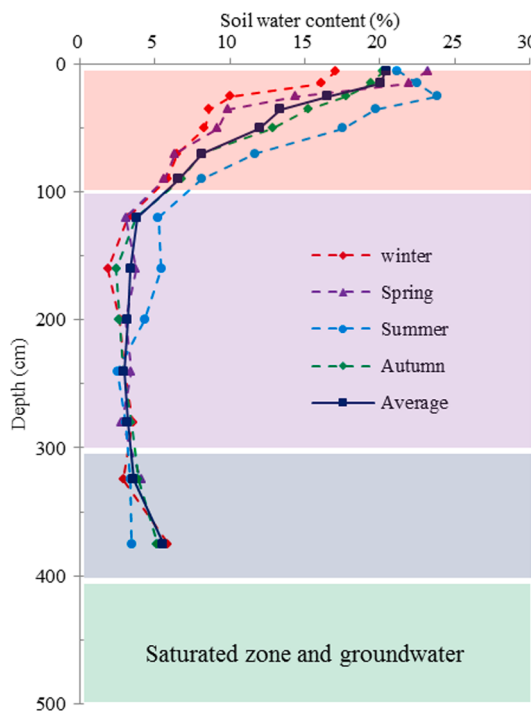


Fig. 7. Soil water content of vadose zone.

autumn, which was attributed to summer precipitation preferentially infiltrating and recharging the deep soil, thereby diluting the chloride concentration.

Soil water $\delta^{18}\text{O}$ values at different soil depths in the vadose zone ranged from $-8.13\text{\textperthousand}$ to $-3.55\text{\textperthousand}$ (Fig. 9), within the range of precipitation $\delta^{18}\text{O}$ in the basin ($-25.18\text{--}3.20\text{\textperthousand}$; Fig. 3). In particular, soil water $\delta^{18}\text{O}$ at depths of 0–40 cm underwent complex changes within a large range under the influence of evaporation and precipitation. At depths of 40–300 cm, soil water $\delta^{18}\text{O}$ fluctuated within a small range, and, at depths of 300–400 cm, it was affected by isotopically depleted groundwater, resulting in relatively low soil water $\delta^{18}\text{O}$ values. Seasonal variations in soil water $\delta^{18}\text{O}$ values of the vadose zone (Fig. 9) indicated that owing to the influence of evaporation, surface soil water had relatively higher $\delta^{18}\text{O}$ values than precipitation in each season (Gazis and Feng, 2004). Furthermore, as precipitation $\delta^{18}\text{O}$ values in winter and spring were relatively low, those of the surface soil water were lower in winter and spring than in summer and autumn (Fig. 9). The soil water

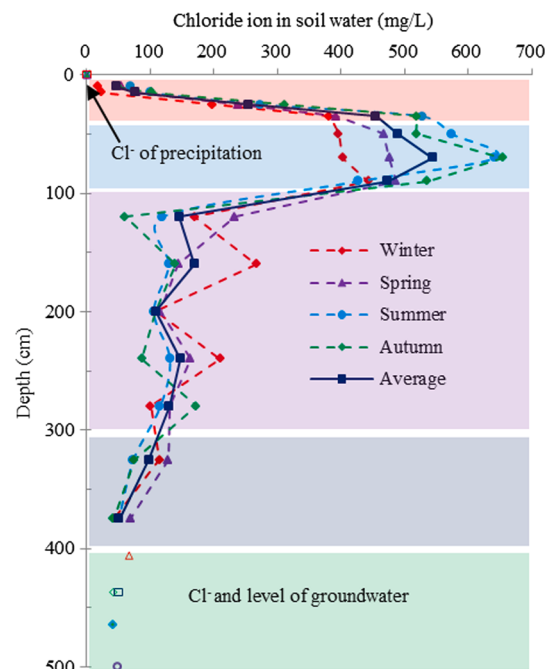


Fig. 8. Chloride concentration of vadose-zone soil water.

$\delta^{18}\text{O}$ values were lower in winter than in other seasons, especially at depths of 0–300 cm, which may have been due to low winter temperatures that led to isotope fractionation during water solidification (Lacelle et al., 2014; Wang et al., 2018). The soil water molecules enriched in heavy oxygen isotopes quickly solidified on the sand grains or rocks, resulting in depleted water $\delta^{18}\text{O}$ in the soil samples.

The soil water content, chloride content, and isotope characteristics varied at different soil profile depths in the *A. splendens* grassland (Figs. 7–9). The main variation characteristics were as follows: under the influence of precipitation and water absorption by plant roots, the soil water content at depths of 0–100 cm gradually decreased with increasing depth, whereas the chloride content gradually increased (similar to depths of 0–400 cm on the Loess Plateau; Li et al., 2017). Due to preferential flow recharge, the chloride content at depths of 100–300 cm was lower than that in the surface layer, and the soil water $\delta^{18}\text{O}$ values fluctuated with increasing depth. Under the influence of groundwater, the soil water content at depths of greater than 300 cm gradually increased with increasing depth, whereas the chloride content gradually decreased.

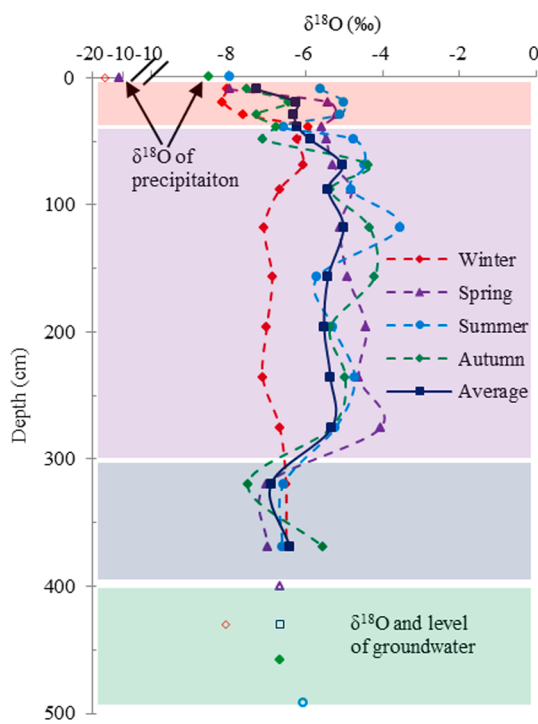


Fig. 9. $\delta^{18}\text{O}$ values of vadose-zone soil water.

4.4. Recharge source and transport mechanism of vadose-zone soil water and groundwater

The range of stable hydrogen and oxygen isotope values in the soil water was covered by that of local precipitation (Figs. 3 and 10), with the $\delta^2\text{H}$ - $\delta^{18}\text{O}$ plots of soil water lying to the lower right of the LMWL (Fig. 10). Furthermore, the local evaporation line of soil water (S-LEL) was $\delta^2\text{H} = 4.74\delta^{18}\text{O} - 20.14$, whose slope (4.74) was lower than that of the LMWL (7.95), as shown in Fig. 10. This indicates that the soil water in this area was mainly influenced by local precipitation, and strong evaporation occurred prior to precipitation infiltration and recharge of the soils (Clark and Fritz, 1997; Gu et al., 2011; Huang et al., 2016). The slope of the S-LEL in each season decreased in the following order: winter (7.57) > spring (5.07) > autumn (4.29) > summer (3.56)

(Fig. 10, Table 1), indicating that the degree of post-precipitation evaporation before infiltration in each season decreased in the following order: summer > autumn > spring > winter. This was mainly controlled by seasonal temperatures (11.7, 0.1, 1.3, and -10.8°C , respectively). The S-LEL slope varied in different soil profile depth ranges (Table 1): 4.15 at 0–40 cm, 4.49 at 40–100 cm, 4.99 at 100–300 cm, and 5.37 at 300–400 cm, and the slope in each depth range was lower than the slope (5.50) of the LEL of groundwater, which indicated that the evaporation intensity of soil water gradually decreased with increasing soil profile depth in the vadose zone (Gazis and Feng, 2004). This was mainly attributed to preferential flow, which was subject to a low degree of evaporation (and thus relatively isotopically depleted), recharging the deep soils and groundwater aquifer more rapidly than piston flow by moving through cracks or plant roots (Xiang et al., 2019). In contrast, piston flow was subject to a high degree of evaporation at the surface, and the S-LEL slope gradually increased downward from the surface.

The CMB method revealed that the mean potential infiltration recharge from precipitation to vadose-zone soil water was 9.20 mm/yr, accounting for 2.17% of the local precipitation. Liu et al. (2010) calculated the precipitation infiltration in the southeastern Badain Jaran

Table 1

Soil water isotope evaporation line in different seasons and depths in the Qinghai Lake Basin.

LEL types	Equations	n	R	P
Soil water in spring	$\delta^2\text{H} = 5.07\delta^{18}\text{O} - 15.67$	14	0.817	$P < 0.001$
Soil water in summer	$\delta^2\text{H} = 3.56\delta^{18}\text{O} - 29.96$	14	0.838	$P < 0.001$
Soil water in autumn	$\delta^2\text{H} = 4.29\delta^{18}\text{O} - 20.87$	14	0.627	$P < 0.02$
Soil water in winter	$\delta^2\text{H} = 7.57\delta^{18}\text{O} - 1.60$	14	0.563	$P < 0.05$
Soil water in depth 0–40 cm	$\delta^2\text{H} = 4.15\delta^{18}\text{O} - 25.59$	16	0.571	$P < 0.05$
Soil water in depth 40–100 cm	$\delta^2\text{H} = 4.49\delta^{18}\text{O} - 22.45$	12	0.801	$P < 0.002$
Soil water in depth 100–300 cm	$\delta^2\text{H} = 4.88\delta^{18}\text{O} - 18.32$	20	0.708	$P < 0.001$
Soil water in depth 300–400 cm	$\delta^2\text{H} = 5.37\delta^{18}\text{O} - 13.56$	8	0.542	–
Groundwater	$\delta^2\text{H} = 5.50\delta^{18}\text{O} - 5.91$	10	0.969	$P < 0.01$

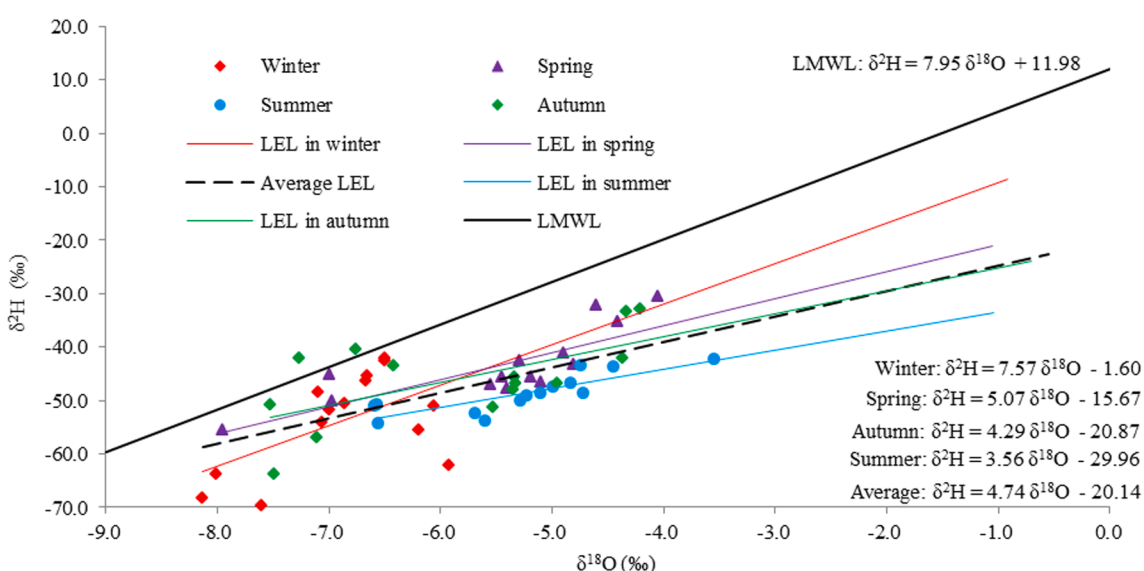


Fig. 10. Stable isotopes and LEL of soil water with the LMWL. LMWL: local meteoric water line; LEL: local evaporation line.

Desert using the chloride tracer method. They found that the annual mean recharge in two research areas were 0.81 mm/yr and 1.24 mm/yr, which accounted for only 0.9% and 1.4% of the multi-year mean annual precipitation, respectively. Wang et al. (2006) calculated the recharge from precipitation infiltration in a typical region of the Hebei Plain using the chloride tracer method. They found that the annual mean recharge in two research areas was 44.72 mm/yr and 31.31 mm/yr, which accounted for 8.2% and 5.8% of the multi-year mean annual precipitation, respectively. These results all indicate that potential recharge from precipitation infiltration varied among regions, which was related to the regional precipitation amount, precipitation intensity, evaporation intensity, surface coverage, and soil structure (Yuan et al., 2015).

The average tritium content at depths of 300–400 cm was 20 TU, which was lower than the peak tritium content (46–72.2 TU in 2014–2015) of vadose-zone soil water at a depth of 600–980 cm in the Loess Plateau (Li et al., 2019; Lu et al., 2020). The tritium content at a depth of 400 cm in the vadose zone of the Loess Plateau was approximately 20 TU (Li et al., 2019). These indicated that the recharge source of groundwater in the studied *A. splendens* grassland was mainly local precipitation since 1963 (after China's nuclear explosion tests in this region), and the vadose-zone soil water is therefore relatively young.

Piston flow and preferential flow likely coexist in hydrological systems (Manna et al., 2017; Xiang et al., 2019; Lu et al., 2020). The source of groundwater recharge comprises both piston and preferential flow, while the chloride content in various water sources is ordered as follows: soil water > groundwater > precipitation (Sharma and Hughes, 1985). In this study, the chloride content of groundwater was 50.25 mg/L, similar to that of deep vadose-zone soil water (51.68 mg/L), greater than that of precipitation (3.02 mg/L), and lower than the average chloride content of vadose-zone soil water (238.06 mg/L). This indicated that the source of groundwater recharge in the research area consisted of preferential flow of precipitation and piston flow of upper soil water. Moreover, groundwater $\delta^{18}\text{O}$ values were significantly lower than those of soil water at a depth of 100 cm but similar to those of precipitation (Fig. 9). Therefore, the preferential flow recharge to groundwater was greater than the piston flow recharge (Li et al., 2017). The CMB method revealed that the annual groundwater recharge from precipitation in the *A. splendens* grassland was 26.29 mm, accounting for approximately 6.19% of the annual precipitation. The average chloride concentrations in precipitation, deep soil water (100–260 cm), and groundwater were 3.02 mg/L, 143.60 mg/L, and 50.25 mg/L, respectively. According to Eqs. (6) and (7), the preferential and piston flow infiltration comprised 66.40% (17.46 mm/yr) and 33.60% (8.83 mm/yr) of the total recharge, respectively. This indicated that the main source of groundwater recharge in the *A. splendens* grassland was preferential flow.

Li et al. (2017) used the chloride tracer method to show that the main source of groundwater in the Loess Plateau was rapid infiltration of precipitation. They found that the total groundwater recharge rate was approximately 107 mm/yr, accounting for 19% of the annual mean precipitation, with preferential flow of precipitation contributing a major fraction (87%), higher than that observed in this study (66.40%). Xiang et al. (2019) showed that the main source of groundwater in the Loess Plateau was piston flow (62%) supplemented by preferential flow (38%). Both of these studies focused on the Loess Plateau but reported different results, suggesting that groundwater recharge mechanisms vary between different geographic sites and are likely controlled by spatial scale, topography, and soil structure (Wiekenkamp et al., 2016). Xiang et al. (2019) pointed out that the generation of preferential flow requires two conditions to be satisfied: namely the occurrence of heavy precipitation and the presence of preferential paths. Precipitation in the *A. splendens* grassland was concentrated in the summer (62.17%). Furthermore, *A. splendens* roots were well-developed, and soil porosity was high (Wang, 2001; Wu et al., 2015), which provided conditions conducive to the development of preferential flow, as confirmed by the relative depletion of heavy isotopes in the groundwater in this study.

5. Conclusion

In this study, we collected samples from the *A. splendens* grassland of the Qinghai Lake Basin for testing and data analysis, revealing the temporal characteristics of local precipitation hydrogen and oxygen isotopes and dustfall chloride. Moreover, we explored the transport mechanism of vadose-zone soil water and estimated the vertical recharge from precipitation to vadose-zone soil water as well as the age of soil water. The results showed that the LMWL of the Qinghai Lake Basin was $\delta^2\text{H} = 7.95\delta^{18}\text{O} + 11.98$. The total annual atmospheric deposition was approximately 279.35 g/m², of which the total chloride deposition was 1.33 g/m², which consisted of precipitation chloride (1.15 g/m²; 86.5%) and dustfall chloride (0.18 g/m²; 13.5%), indicating that the former was the main source of chloride input to the area.

Soil water content, chloride content, and isotope characteristics in the soil profile of the *A. splendens* grassland varied at different depths. Due to precipitation and water absorption by plant roots, soil water content at depths of 0–100 cm gradually decreased with increasing depth, whereas chloride content gradually increased. Due to preferential flow recharge, the chloride content at depths of 100–300 cm was lower than that at the surface layer; soil water $\delta^{18}\text{O}$ values fluctuated in this depth range. Under the influence of groundwater, soil water content at depths of more than 300 cm gradually increased with increasing depth, concomitant with a gradual decrease in chloride content.

The annual mean potential infiltration recharge from precipitation to soil water in the vadose zone profile was 9.20 mm/yr, which accounted for 2.17% of the local precipitation. The annual groundwater recharge from precipitation was 26.29 mm and accounted for about 6.19% of the annual precipitation, with preferential and piston flow infiltration contributing 66.40% (17.46 mm/yr) and 33.60% (8.83 mm/yr) of the total recharge, respectively. This indicated that the main source of groundwater recharge in the study area was preferential flow. Groundwater recharge mechanisms varied between different regions and were controlled by factors such as spatial scale, topography, and soil structure.

Declaration of Competing Interest

The authors declare that they have no known competing financial interests or personal relationships that could have appeared to influence the work reported in this paper.

Acknowledgements

The study was supported by the National Natural Science Foundation of China (41730854, 41877157, 41530854); the Project supported by State Key Laboratory of Loess and Quaternary Geology (SKLLQG1904); the Science and technology support plan for Youth Innovation of colleges and universities of Shandong (2019KJH009); the Natural Science Foundation of Shandong Province (ZR2019MD040); the Key Research and Development Plan of Shandong Province (2018GSF117021); the Science and technology program of colleges and universities of Shandong (J17KA192); and the Project supported by State Key Laboratory of Earth Surface Processes and Resource Ecology (2017-KF-15).

References

- Adomako, D., Maloszewski, P., Stumpp, C., 2010. Estimating groundwater recharge from water isotope ($\delta^2\text{H}$, $\delta^{18}\text{O}$) depth profiles in the Densu River basin Ghana. *Hydrol. Sci. J.* 55 (8), 1405–1416.
- Allison, G.B., Hughes, M.W., 1983. The use of natural tracers as indicators of soil-water movement in a temperate semi-arid region. *J. Hydrol.* 60 (1), 157–173.
- Baran, N., Richert, J., Mouvet, C., 2007. Field data and modelling of water and nitrate movement through deep unsaturated loess. *J. Hydrol.* 345, 27–37.
- Bashir, R., Chevez, E.P., 2018. Spatial and seasonal variations of water and salt movement in the vadose zone at salt-impacted sites. *Water* 10 (12), 1833.
- Chen, G.C., Chen, X.Q., Gou, X.J., 2008. Ecological Environment Protection and Restoration in Qinghai Lake Basin. Qinghai People Press, Qinghai (in Chinese).

- Clark, I.D., Fritz, P., 1997. Environmental Isotopes in Hydrogeology. Lewis Publishers, New York.
- Cui, B.L., Li, X.Y., 2015. Stable isotopes reveal sources of precipitation in the Qinghai Lake Basin of the northeastern Tibetan Plateau. *Sci. Total Environ.* 527–528, 26–37.
- Cui, B.L., Li, X.Y., 2016. Isotope and hydrochemistry reveal evolutionary processes of lake water in Qinghai Lake. *J. Great Lakes Res.* 42, 580–587.
- Edmunds, W., Tyler, S., 2002. Unsaturated zones as archives of past climates: toward a new proxy for continental regions. *Hydrogeol. J.* 10 (1), 216–228.
- Favreau, G., Cappaer, B., Massuel, S., Leblanc, M., Boucher, M., Boulain, M., Leduc, G., 2009. Land clearing, climate variability, and water resources increase in semiarid southwest Niger: a review. *Water Resour. Res.* 45, 1–18.
- Gao, G.S., Song, L.M., Ma, Z.T., 2013. Temporal-spatial distribution and impact factors of dust fall in Qinghai Province of China. *J. Desert Res.* 33 (4), 1124–1130 (in Chinese).
- Gao, Y.X., Zhang, B., Cui, H.H., 2014. A study of the migration of chemical compositions in vadose water infiltration. *Hydrogeol. Eng. Geol.* 41 (2), 1–6 (in Chinese).
- Gazis, C., Feng, X.H., 2004. A stable isotope study of soil water: evidence for mixing and preferential flow paths. *Geoderma* 119, 97–111.
- Gibson, J.J., Edwards, T.W.D., Birks, S.J., Amour, N.A.S., Buhay, W.M., WeEachern, P., Wolfe, B.B., Peters, D.L., 2005. Progress in isotope tracer hydrology in Canada. *Hydrog. Process.* 19, 303–327.
- Gleeson, T., Befus, K.M., Jasechko, S., Luijendijk, E., Cardenas, M.B., 2016. The global volume and distribution of modern groundwater. *Nat. Geosci.* 9, 161–167.
- Goldin, T., 2016. Groundwater: India's drought below ground. *Nat. Geosci.* 9, 98.
- Gu, W.Z., Pang, Z.H., Wang, Q.J., 2011. Isotope Hydrology. Science Press, Beijing (in Chinese).
- Gui, J., Li, Z.S., Feng, Q., Wei, W., Li, Y.G., Lv, Y.M., Yuan, R.F., Zhang, B.J., 2019. Space-time characteristics and environmental significance of the stable isotopes in precipitation in the Gulang River Basin. *Environ. Sci.* 40 (1), 149–156 (in Chinese).
- Herczeg, A.L., Leaney, F.W., 2011. Review: environmental tracers in arid-zone hydrology. *Hydrogeol. J.* 19 (1), 17–29.
- Hou, S.B., Song, X.F., Yu, J.J., Liu, X., Zhang, G.Y., 2008. Stable isotope characteristics in the process of precipitation and infiltration in Taihang Mountainous Region. *Resour. Sci.* 30 (1), 86–92 (in Chinese).
- Huang, T.M., Yang, S., Liu, J.L., Li, Z., 2016. How much information can soil solute profiles reveal about groundwater recharge? *Geosci. J.* 20 (4), 495–502.
- IAEA (International Atomic Energy Agency), 2013. Isotope methods for dating old groundwater. Vienna, Austria.
- Kendall, C., McDonnell, J.J., 1998. Isotope Tracer in Catchment Hydrology. Elsevier, New York, pp. 155–158.
- Lacelle, D., Fontaine, M., Forest, A.P., Kokelj, S., 2014. High-resolution stable water isotopes as tracers of thaw unconformities in permafrost: a case study from western Arctic Canada. *Chem. Geol.* 368, 85–96.
- Li, X.Y., Xu, H.Y., Sun, Y.L., Zhang, D.S., Yang, Z.P., 2007. Lake-level change and water balance analysis at Lake Qinghai, west China during recent decades. *Water Resour. Manage.* 21, 1505–1516.
- Li, X.Y., Yang, X.F., Ma, Y.J., Hu, X., Wang, P., Huang, Y.M., Cui, B.L., Wei, J.Q., 2018. Qinghai lake basin critical zone observatory on the Qinghai-Tibet Plateau. *Vadose Zone J.* 17, 180069.
- Li, Z., Chen, X., Liu, W.Z., Si, B.C., 2017. Determination of groundwater recharge mechanism in the deep loessial unsaturated zone by environmental tracers. *Sci. Total Environ.* 586, 827–835.
- Li, Z., Jasechko, S., Si, B.C., 2019. Uncertainties in tritium mass balance models for groundwater recharge estimation. *J. Hydrol.* 571, 150–158.
- Lin, D., Jin, M.G., Liang, X., Zhao, H.B., 2013. Estimating groundwater recharge beneath irrigated farmland using environmental tracers fluoride, chloride and sulfate. *Hydrogeol. J.* 21 (7), 1469–1480.
- Liu, J., Wei, W., Zhang, L., Wang, Y., Duan, B.X., Liu, F.L., 2012. The application of δD and $\delta^{18}\text{O}$ isotopes of soil water in revealing the water transport in the inclusion zone. *Surv. Sci. Technol.* 5, 38–43 (in Chinese).
- Liu, J.R., Song, X.F., Yuan, G.F., Sun, X.M., Liu, X., Chen, F., Wang, Z.M., Wang, S.Q., 2008. Characteristics of $\delta^{18}\text{O}$ in precipitation over northwest China and its water vapor sources. *Acta Geograph. Sin.* 63 (1), 12–22 (in Chinese).
- Liu, X.Y., Chen, J.S., Sun, X.X., 2010. Application of chloride tracer method to study replenishment ratio of precipitation in desert. *Trans. Chin. Soc. Agric. Eng.* 26 (S1), 146–149.
- Lu, Y.W., Li, H.J., Si, B.C., Li, M., 2020. Chloride tracer of the loess unsaturated zone under sub-humid region: a potential proxy recording high-resolution hydroclimate. *Sci. Total Environ.* 700, 134465.
- Ma, J.Z., Chen, F.H., Zhao, H., 2004. Unsaturated zone records of groundwater recharge and climate change in Badain Jaran desert since 1000 years ago. *Chin. Sci. Bull.* 49 (1), 22–24 (in Chinese).
- Manna, F., Walton, K.M., Cherry, J.A., Parker, B.L., 2017. Mechanisms of recharge in a fractured porous rock aquifer in a semi-arid region. *J. Hydrol.* 555, 869–880.
- Reck, A., Paton, E., Kluge, B., 2018. Advanced in situ soil water sampling system for monitoring solute fluxes in the vadose zone. *Vadose Zone J.* 18 (1), 190008.
- Scanlon, B.R., Keese, K.E., Flint, A.L., Flint, L.E., Gaye, C.B., Edmunds, W.M., Simmers, I., 2006. Global synthesis of groundwater recharge in semiarid and arid regions. *Hydrog. Process.* 20 (15), 3335–3370.
- Scanlon, B.R., Mukherjee, A., Gates, J., Reedy, R.C., Sinha, A.K., 2010. Groundwater recharge in natural dune system sand agricultural ecosystems in the Thar Desert region, Rajasthan India. *Hydrogeol. J.* 18 (4), 959–972.
- Scanlon, B.R., Reedy, R.C., Tachovsky, J.A., 2007. Semiarid unsaturated zone chloride profiles: Archives of past land use change impacts on water resources in the southern High Plains United States. *Water Resour. Res.* 43 (6), W06423.
- Sharma, M.L., Hughes, M.W., 1985. Groundwater recharge estimation using chloride, deuterium and oxygen-18 profiles in the deep coastal sands of western Australia. *J. Hydrol.* 81, 93–109.
- Tan, H.B., Wen, X.W., Rao, W.B., John, B., Huang, J.Z., 2016. Temporal variation of stable isotopes in a precipitation-groundwater system: implications for determining the mechanism of groundwater recharge in high mountain-hills of the Loess Plateau, China. *Hydrog. Process.* 30, 1491–1505.
- Tang, M.C., Gao, X.Q., Zhang, J., 1992. The annual changes of the water level of the Lake Qinghai in the recent thirty years. *Chin. Sci. Bull.* 37 (6), 524–527 (in Chinese).
- Tian, L.D., Yao, T.D., Sun, W.Z., Stievenard, M., Jouzel, J., 2001. Relationship between δD and $\delta^{18}\text{O}$ in precipitation on north and south of the Tibetan Plateau and moisture recycling. *Sci. China* 44 (9), 789–796.
- Wan, D.J., Jin, Z.D., Wang, Y.X., 2012. Geochemistry of eolian dust and its elemental contribution to Lake Qinghai sediment. *Appl. Geochem.* 27, 1546–1555.
- Wang, B.G., Jin, M.G., Wang, W.F., 2006. Application of chloride ion tracer method in evaluation of groundwater recharge in vertical infiltration in Hebei Plain. *Water-saving Irrig.* 3, 16–20 (in Chinese).
- Wang, K., 2001. Study of *Achnatherum splendens* grass on the function of soil and water conservation. *Res. Soil Water Conserv.* 8 (2), 157–159 (in Chinese).
- Wang, S.Q., Song, X.F., Xia, G.Q., Wang, Z.M., Liu, X., Wang, P., 2009. Application of oxygen and hydrogen isotope in the process of precipitation infiltration in the shallow groundwater areas of North China Plain. *Adv. Water Sci.* 20 (4), 495–501 (in Chinese).
- Wang, W.H., Wu, T.H., Zhao, L., Li, R., Zhu, X.F., Wang, W.R., Yang, S.H., Qin, Y.H., Hao, J.M., 2018. Exploring the ground ice recharge near permafrost table on the central Qinghai-Tibet Plateau using chemical and isotopic data. *J. Hydrol.* 560, 220–229.
- Wiekenkamp, I., Huisman, J.A., Bogen, H.R., Lin, H.S., Vereecken, H., 2016. Spatial and temporal occurrence of preferential flow in a forested headwater catchment. *J. Hydrol.* 534, 139–149.
- Wu, H.W., Li, X.Y., Jiang, Z.Y., Li, J., Zheng, X.R., Zhao, D.Z., 2015. Variations in water use for *Achnatherum splendens* in Lake Qinghai watershed, based on δD and $\delta^{18}\text{O}$. *Acta Ecol. Sin.* 35 (24), 1552–1564 (in Chinese).
- Xiang, W., Si, B.C., Biswas, A., Li, Z., 2019. Quantifying dual recharge mechanisms in deep unsaturated zone of Chinese Loess Plateau using stable isotopes. *Geoderma* 337, 773–781.
- Xin, H., 2008. A green fervor sweeps the Qinghai-Tibetan Plateau. *Science* 321, 633–635.
- Xu, S.G., Liu, Y.F., Sun, W.G., 2006. Research on the stable isotope for soil water vertical transporting in unsaturated zone of Zhalong Wetland. *J. China Hydrol.* 26 (5), 1–6 (in Chinese).
- Ye, R.Z., Chang, J., 2019. Study of groundwater in permafrost regions of China: status and process. *J. Glaciol. Geocryol.* 41 (1), 183–196 (in Chinese).
- Yu, W.S., Yao, T.D., Tian, L.D., Ma, Y.M., Ichiyanagi, K., Wang, Y., Sun, W.Z., 2008. Relationships between $\delta^{18}\text{O}$ in precipitation and air temperature origin on a south-north transect of the Tibetan Plateau. *Atmos. Res.* 87, 158–169.
- Yuan, R.Q., Long, X., Wang, P., Song, X.F., 2015. GPU parallel computing and fast simulation of distributed hydrological models. *J. China Hydrol.* 35 (4), 7–13 (in Chinese).
- Zhang, H.Q., Peng, M., Wang, B., Lu, W.Z., Gao, Y.H., Du, T.Y., 2006. The present situation and cause analysis of ecological environment deterioration in Qinghai Lake. *J. Qinghai Environ.* 16 (2), 51–56 (in Chinese).
- Zhao, G.Q., Li, X.Y., Wu, H.W., Zhang, S.Y., Li, G.Y., 2013. Study on plant water use in *Myricaria squamosa* with stable hydrogen isotope tracer in Qinghai Lake basin. *Chin. J. Plant Ecol.* 37 (12), 1091–1100 (in Chinese).
- Zhou, G.Y., Chen, G.C., Zhao, Y.L., 2003. Study on *Achnatherum splendens* community characteristics and species diversity around Qinghai Lake. *Acta Bot. Boreali-Occidentalis Sin.* 11, 1955–1961 (in Chinese).
- Zhu, Y.J., Jia, X.X., Qiao, J.B., Binley, A., Horton, R., Hu, W., Wang, Y.Q., Shao, M.A., 2019. Capacity and distribution of water stored in the vadose zone of the Chinese Loess Plateau. *Vadose Zone J.* 18 (1), 180203.